

Stable evaluation of derivatives for barycentric and continued fraction representations of rational functions

Tobin A. Driscoll^{1*} and Yuxing Zhou^{1†}

¹Department of Mathematical Sciences, University of Delaware, Newark, 19716, DE, USA.

*Corresponding author(s). E-mail(s): driscoll@udel.edu;
Contributing authors: zhouyx@udel.edu;

†These authors contributed equally to this work.

Abstract

Fast algorithms for approximation by rational functions exist for both barycentric and Thiele continued fraction (TCF) representations. We present the first numerically stable methods for derivative evaluation in the barycentric representation, including an $O(n)$ algorithm for all derivatives. We also extend an earlier $O(n)$ algorithm for evaluation of the TCF first derivative to higher orders. Numerical experiments confirm the robustness and efficiency of the proposed methods.

Keywords: approximation, barycentric representation, continued fractions, numerical stability

1 Introduction

Interest in computational approximation of functions by rational functions has grown since the advent of the AAA algorithm [1], which has found applications in model reduction, constructive approximation, PDEs, and more, as surveyed by Nakatsukasa and Trefethen [2]. The AAA algorithm computes an SVD to find weights for the barycentric interpolation representation of a rational function, thereby minimizing a linearized approximation error. This approach is embedded within a greedy iteration for selecting new interpolation nodes. More recently, a similar greedy approach to node selection using Thiele continued fraction (TCF) interpolation was suggested and demonstrated by Salazar Celis [3] and shown to be 3–10 times faster than AAA to construct by Driscoll and Zhou [4]. Both AAA and greedy TCF produce interpolants on n nodes that can be evaluated stably in $O(n)$ elementary operations.

Derivatives of rational approximants are useful in many applications. For barycentric rational interpolants, Schneider and Werner [5] gave $O(n)$ formulas for the derivatives—one for a generic point, and a different one at nodes. However, the generic formula is numerically unstable near nodes [2]. For TCF interpolants, Driscoll and Zhou [4] gave an $O(n)$ iterative formula for the first derivative based on forward-mode automatic differentiation without investigation of its numerical stability.

In this work, we present a double-summation formula for the first derivative of the barycentric representation that removes the dominant cancellation error but requires $O(n^2)$ operations. We then derive a modified $O(n)$ algorithm for all derivatives that avoids the dominant cancellation. For TCF interpolants, we show that the $O(n)$ iterative formula given

by Driscoll and Zhou [4] is stable in practice and straightforward to generalize to higher derivatives.

The rest of this paper is organized as follows. In [section 2](#), we review the barycentric representation and the original formula of Schneider and Werner for its derivative. We point out the source of subtractive cancellation and then present methods that avoid it. In [section 3](#), we review the Thiele continued fraction representation and the iteration of Driscoll and Zhou to compute its first derivative, which we then generalize to higher-order derivatives. Numerical experiments are reported in [section 4](#), and conclusions are drawn in [section 5](#).

2 Barycentric representation

The barycentric representation of a rational function with n distinct nodes z_1, z_2, \dots, z_n is

$$r(z) = \frac{\sum_{k=1}^n \frac{w_k f_k}{z - z_k}}{\sum_{k=1}^n \frac{w_k}{z - z_k}} = \frac{N(z)}{D(z)}, \quad (1)$$

where $f_k = f(z_k)$ are interpolated function values at the nodes and w_k are the barycentric weights, which can be used to improve approximation properties.

Implicit differentiation of $r(z)D(z) = N(z)$ leads to

$$r'(z) = \frac{N'(z) - r(z)D'(z)}{D(z)}. \quad (2)$$

This formula was suggested by Schneider and Werner [5] for computing the first derivative of a barycentric representation at points other than nodes. However, it is numerically unstable when z is close to one of the nodes, say z_j . Define $\epsilon = z - z_j$ and

$$N_j(z) = \sum_{\substack{k=1 \\ k \neq j}}^n \frac{w_k f_k}{z - z_k}, \quad D_j(z) = \sum_{\substack{k=1 \\ k \neq j}}^n \frac{w_k}{z - z_k}. \quad (3)$$

We expand

$$r(z) = \left[\frac{w_j f_j}{\epsilon} + N_j(z) \right] \left[\frac{w_j}{\epsilon} + D_j(z) \right]^{-1} \quad (4)$$

$$= \left[f_j + \frac{\epsilon}{w_j} N_j(z) \right] \left[1 + \frac{\epsilon}{w_j} D_j(z) \right]^{-1} \quad (5)$$

$$= f_j + \frac{N_j - f_j D_j}{w_j} \epsilon + O(\epsilon^2). \quad (6)$$

Thus,

$$N'(z) - r(z)D'(z) = \left[\frac{-w_j f_j}{\epsilon^2} - N'_j(z) \right] - \left[f_j + O(\epsilon) \right] \left[\frac{-w_j}{\epsilon^2} - D'_j(z) \right], \quad (7)$$

which requires an unstable subtractive cancellation of the dominant terms. [Figure 1](#) illustrates the result of this subtractive cancellation when the rational function r is an AAA approximation to $f(x) = e^x$ on $[-1, 1]$ of type $(5, 5)$, accurate to within 5×10^{-13} . The error in evaluating $r'(x)$ using (2) grows as x approaches the node at 0.75, reaching about 0.034 at a distance of 10^{-14} from the node.

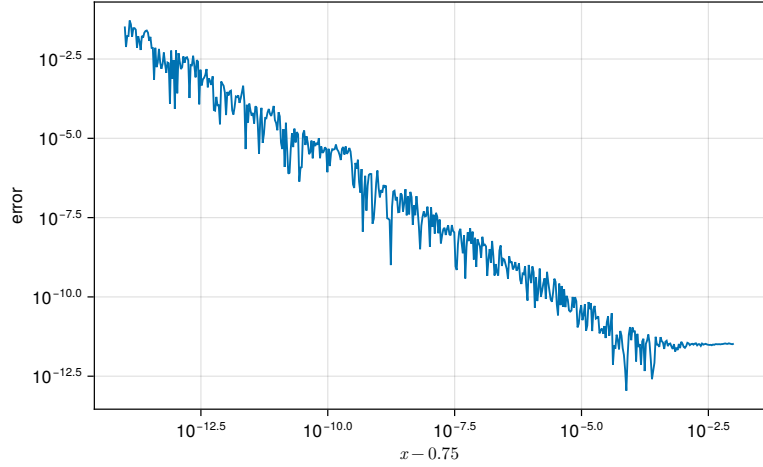


Fig. 1 Absolute error near a node using (2) to evaluate the first derivative of an AAA rational approximation $r(x)$ to $f(x) = e^x$ on $[-1, 1]$. The approximation to f is of type $(5, 5)$ and accurate to within 5×10^{-13} , but due to subtractive cancellation, the evaluation of $r'(x)$ grows when approaching the node 0.75.

One way to avoid the cancellation instability is to multiply (2) through by D and rewrite the numerator as the double sum

$$N'(z)D(z) - N(z)D'(z) = \sum_{j=1}^n \sum_{k=1}^n \frac{w_j w_k (f_k - f_j)}{(z - z_j)^2 (z - z_k)}. \quad (8)$$

Numerical experiments confirm that this formula resolves the instability, but since it has $O(n^2)$ complexity, we next suggest an alternative that is $O(n)$.

Consider the representation $r = \tilde{N}/\tilde{D}$, with

$$\tilde{N}(z) = \epsilon N(z), \quad \tilde{D}(z) = \epsilon D(z), \quad (9)$$

still using $\epsilon = z - z_j$. Then

$$r'(z) = \frac{\tilde{N}'(z) - r(z)\tilde{D}'(z)}{\tilde{D}(z)}. \quad (10)$$

Expanding this numerator leads to

$$\tilde{N}'(z) - r(z)\tilde{D}'(z) = [N_j(z) + \epsilon N'_j(z)] - [f_j + O(\epsilon)][D_j(z) + \epsilon D'_j(z)], \quad (11)$$

which has no intrinsic subtractive cancellation. Hence, we can use (10) stably instead of (2) at all points that are close to z_j . Note that as $z \rightarrow z_j$, we obtain

$$r'(z_j) = \frac{N_j(z_j) - f_j D_j(z_j)}{w_j} = \frac{1}{w_j} \sum_{k=1, k \neq j}^n \frac{w_k (f_k - f_j)}{z_j - z_k}, \quad (12)$$

which is the Schneider–Werner alternate formula for the derivative at a node.

For higher-order derivatives, we can apply Leibniz's product rule formula to $r\tilde{D} = \tilde{N}$ and solve to obtain

$$r^{(m)}(z) = \frac{1}{\tilde{D}(z)} \left[\tilde{N}^{(m)}(z) - \sum_{k=1}^m \binom{m}{k} r^{(m-k)}(z) \tilde{D}^{(k)}(z) \right], \quad m \geq 1, \quad (13)$$

where

$$\tilde{N}^{(m)}(z) = \epsilon N^{(m)}(z) + m N^{(m-1)}(z), \quad \tilde{D}^{(m)}(z) = \epsilon D^{(m)}(z) + m D^{(m-1)}(z). \quad (14)$$

In general, when evaluating the derivative at a point z , we can find the index j of the node closest to z in $O(n)$ time and use the modified formula (10) with $\epsilon = z - z_j$. An outline for evaluation of barycentric derivatives is given in [Algorithm 1](#).

Algorithm 1 Stable evaluation of derivatives of barycentric rational functions

Require: Evaluation point ζ , max derivative order μ , and n -vectors of nodes z , function values f , and weights w

- 1: $\delta_k \leftarrow \zeta - z_k, \quad k = 1, 2, \dots, n$
- 2: $j \leftarrow \arg \min_k |\delta_k|$
- 3: $N_j^{(m)} \leftarrow 0, D_j^{(m)} \leftarrow 0, \quad m = 0, 1, \dots, \mu$
- 4: **for** $k = 1, \dots, n$, except j **do** \triangleright Calculate N_j and D_j from (3), and their derivatives
- 5: $d \leftarrow w_k / \delta_k$
- 6: Add $f_k d$ to $N_j^{(0)}$
- 7: Add d to $D_j^{(0)}$
- 8: **for** $m = 1, \dots, \mu$ **do**
- 9: $d \leftarrow -md / \delta_k$
- 10: Add $f_k d$ to $N_j^{(m)}$
- 11: Add d to $D_j^{(m)}$
- 12: $\tilde{N}^{(0)} \leftarrow w_k f_k + \delta_j N_j^{(0)}$
- 13: $\tilde{D}^{(0)} \leftarrow w_k + \delta_j D_j^{(0)}$
- 14: $r^{(0)} \leftarrow \tilde{N}^{(0)} / \tilde{D}^{(0)}$
- 15: **for** $m = 1, \dots, \mu$ **do** \triangleright Apply (13) and (14)
- 16: $\tilde{N}^{(m)} \leftarrow m N_j^{(m-1)} + \delta_j N_j^{(m)}$
- 17: $\tilde{D}^{(m)} \leftarrow m D_j^{(m-1)} + \delta_j D_j^{(m)}$
- 18: $r^{(m)} \leftarrow \left[\tilde{N}^{(m)} - \sum_{j=1}^m \binom{m}{j} r^{(m-j)} \tilde{D}^{(j)} \right] / \tilde{D}^{(0)}$
- 19: **return** $r^{(0)}, r^{(1)}, \dots, r^{(\mu)}$

3 Continued fraction representation

The Thiele continued fraction (TCF) representation of a rational function with n distinct nodes z_1, z_2, \dots, z_n is

$$r(z) = w_1 + \cfrac{z - z_1}{w_2 + \cfrac{z - z_2}{w_3 + \dots \cfrac{z - z_{n-1}}{w_n}}}. \quad (15)$$

The TCF coefficients w_k (which are unrelated to the weights in the barycentric formula) can be computed iteratively for $k = 1, \dots, n$ through

$$\begin{aligned} t_1 &= f_k, \\ t_{i+1} &= \frac{z_k - z_i}{-w_i + t_i}, \quad i = 1, 2, \dots, k-1, \\ w_k &= t_k, \end{aligned} \quad (16)$$

Jones and Thron [6] recommended the tail-ordered evaluation of $r(z)$. In terms of the standard generic continued fraction expression

$$r(z) = b_0 + \cfrac{a_1}{b_1 + \cfrac{a_2}{b_2 + \dots \cfrac{a_{n-2}}{b_{n-1} + \cfrac{a_n}{b_n}}}}, \quad (17)$$

the evaluation procedure is

$$\begin{aligned} u_{n+1} &= 0, \\ u_k &= \cfrac{a_k}{b_k + u_{k+1}}, \quad k = n, n-1, \dots, 1, \\ r(z) &= u_0 = b_0 + u_1. \end{aligned} \quad (18)$$

Driscoll and Zhou, however, found [4] that an alternative iteration was faster in floating-point arithmetic, due to requiring just a single division:

$$\begin{aligned} \begin{bmatrix} p_{n+1} \\ q_{n+1} \end{bmatrix} &= \begin{bmatrix} 1 \\ 0 \end{bmatrix}, \\ \begin{bmatrix} p_k \\ q_k \end{bmatrix} &= \begin{bmatrix} b_k p_{k+1} + q_{k+1} \\ a_k p_{k+1} \end{bmatrix}, \quad k = n, n-1, \dots, 1, \\ \begin{bmatrix} p_0 \\ q_0 \end{bmatrix} &= \begin{bmatrix} b_0 p_1 + q_1 \\ p_1 \end{bmatrix}, \\ r(z) &= \frac{p_0}{q_0}. \end{aligned} \quad (19)$$

We now show that these alternatives have the same numerical stability.

Theorem 1 *Using the standard model of floating-point arithmetic and stability [7], the iterations (18) and (19) have the same stability.*

Proof First, we establish that $u_k = q_k/p_k$ in exact arithmetic for $k = 1, \dots, n$. This is trivial for $k = n+1$. For $k = n, n-1, \dots, 1$, we have by induction that

$$\frac{q_k}{p_k} = \frac{a_k p_{k+1}}{b_k p_{k+1} + q_{k+1}} = \frac{a_k p_{k+1}}{b_k p_{k+1} + u_{k+1} p_{k+1}} = u_k. \quad (20)$$

Multiplications and divisions in floating-point have condition number 1 and do not affect stability. By (20), the addition step $b_k p_{k+1} + q_{k+1}$ in (19) is a multiple p_{k+1} of the addition $b_k + u_{k+1}$ in (18), so that step has the same relative condition number in both algorithms. \square

Both (18) and (19) are easily differentiated using forward-mode automatic differentiation. Driscoll and Zhou [4] gave the algorithm based on (19) for the first derivative, which we extend in [Algorithm 2](#) to higher derivatives. Defining $b_k = w_{k+1}$ and $a_k = z - z_k$, and stopping one term earlier in (17), we note that the m th derivatives of p_k and q_k satisfy the recurrences

$$p_k^{(m)} = w_{k+1} p_{k+1}^{(m)} + q_{k+1}^{(m)}, \quad (21)$$

$$q_k^{(m)} = (z - z_k) p_{k+1}^{(m)} + m p_{k+1}^{(m-1)}, \quad (22)$$

initialized by $p_n^{(m)} = q_n^{(m)} = 0$ for $m > 0$, and $p_n^{(0)} = 1$, $q_n^{(0)} = 0$. For the final iteration with $k = 0$, the first equation is the same, and $q_0^{(m)} = p_1^{(m)}$. The derivatives of r then follow as in (13), with p and q replacing \tilde{N} and \tilde{D} .

Algorithm 2 Evaluation of a Thiele continued fraction and its derivatives.

Require: Evaluation point ζ , max derivative order μ , and n -vectors of nodes z and weights

```

 $p_n^{(0)} \leftarrow 1, q_n^{(0)} \leftarrow 0$ 
 $w$ 
 $p_n^{(m)} \leftarrow 0, q_n^{(m)} \leftarrow 0$  for  $m = 1, \dots, \mu$ 
for  $k = n - 1, \dots, 1$  do
   $p_k^{(0)} \leftarrow w_{k+1}p_{k+1}^{(0)} + q_{k+1}^{(0)}$ 
   $q_k^{(0)} \leftarrow (\zeta - z_k)p_{k+1}^{(0)}$ 
  for  $m = 1, \dots, \mu$  do
     $p_k^{(m)} \leftarrow w_{k+1}p_{k+1}^{(m)} + q_{k+1}^{(m)}$ 
     $q_k^{(m)} \leftarrow (\zeta - z_k)p_{k+1}^{(m)} + mp_{k+1}^{(m-1)}$ 
   $p_0^{(0)} \leftarrow w_1p_1^{(0)} + q_1^{(0)}, q_0^{(0)} \leftarrow p_1^{(0)}$ 
   $r^{(0)} \leftarrow p_0^{(0)} / q_0^{(0)}$ 
for  $m = 1, \dots, \mu$  do
   $p_0^{(m)} \leftarrow w_1p_1^{(m)} + q_1^{(m)}$ 
   $q_0^{(m)} \leftarrow p_1^{(m)}$ 
   $r^{(m)} \leftarrow \left[ p_0^{(m)} - \sum_{j=1}^m \binom{m}{j} r^{(m-j)} q_0^{(j)} \right] / q_0^{(0)}$ 
return  $r^{(0)}, r^{(1)}, \dots, r^{(\mu)}$ 

```

Function	Characteristics
$f_E(x) = c \cdot \exp(\sin(x))$	Entire function
$f_C(x) = c \cdot \cos(20x)$	Highly oscillatory
$f_T(x) = c \cdot \tanh(x/\epsilon)$	Meromorphic with nearest poles at $\pm i\pi\epsilon/2$
$f_L(x) = c \cdot \log(1 + \epsilon - x)$	Branch point at $1 + \epsilon$
$f_A(x) = c \cdot \arctan(x/\epsilon)$	Branch points at $\pm i\epsilon$

Table 1 Test functions used in numerical experiments on the interval $[-1, 1]$. The scaling constant c is always chosen so that $\|f^{(m)}\|_\infty = 1$ over the domain, where m is the derivative order being tested.

Function	Characteristics
$f_E(z) = c \cdot \exp(\sin(z))$	Entire function
$f_O(z) = c \cdot \cos(z^{10})$	Highly oscillatory
$f_L(z) = c \cdot \log(1 + \epsilon - z)$	Branch point at $1 + \epsilon$
$f_S(z) = c \cdot \sqrt{1 - \left(\frac{1-\epsilon}{z}\right)^2}$	Branch points at $\pm(1 - \epsilon)$
$f_M(z) = c \tan(z^{-4})$	Meromorphic with essential singularity at 0

Table 2 Test functions used in numerical experiments on the unit circle. The scaling constant c is always chosen so that $\|f^{(m)}\|_\infty = 1$ over the domain, where m is the derivative order being tested.

4 Numerical experiments

We have implemented [Algorithm 1](#) and [Algorithm 2](#) in version 0.3.2 of the RationalFunctionApproximation.jl package [8] for the Julia programming language. Here, we report the results of tests of these implementations on the functions listed in [Table 1](#) over the interval $[-1, 1]$ and the functions listed in [Table 2](#) on the unit circle. Each function f is scaled so the derivative being measured has max-norm 1 over the domain of interest.

For each test function f , we construct a rational approximant r using the continuum AAA algorithm [9] or continuum greedy TCF [4] to a target accuracy of 100 times machine epsilon. We then construct a test set T_f consisting of the union of the following sets:

- 5000 uniformly spaced points in the domain,

Function		Barycentric			TCF		
Name	ϵ	Formula	Formula-EP	Direct	Formula	Formula-EP	Direct
f_E	—	1.507e-13	1.476e-13	7.494e-14	8.640e-13	8.640e-13	2.034e-13
f_C	—	4.474e-14	4.188e-14	1.618e-13	5.916e-12	2.039e-12	7.605e-14
f_T	10^{-2}	1.453e-13	1.451e-13	2.185e-13	4.648e-14	4.638e-14	1.930e-13
f_T	10^{-4}	4.902e-11	5.282e-11	2.110e-14	5.852e-13	2.425e-13	3.587e-14
f_T	10^{-6}	3.934e-07	3.934e-07	2.146e-13	2.101e-08	2.125e-08	1.333e-13
f_L	10^{-2}	4.086e-11	4.077e-11	3.900e-14	2.453e-11	2.453e-11	4.441e-16
f_L	10^{-4}	6.081e-11	6.071e-11	4.108e-15	2.854e-11	2.851e-11	3.331e-16
f_L	10^{-6}	9.653e-09	9.654e-09	1.299e-14	5.952e-12	5.961e-12	3.331e-16
f_A	10^{-2}	8.954e-13	8.906e-13	3.855e-14	2.356e-13	2.363e-13	5.107e-15
f_A	10^{-4}	1.077e-08	1.077e-08	7.050e-15	2.619e-12	2.602e-12	6.251e-14
f_A	10^{-6}	5.575e-09	5.575e-09	4.607e-14	8.948e-09	8.950e-09	1.543e-14

Table 3 Experimental results for the interval $[-1, 1]$ and derivative order $m = 1$.

Function		Barycentric			TCF		
Name	ϵ	Formula	Formula-EP	Direct	Formula	Formula-EP	Direct
f_E	—	1.912e-11	1.484e-11	1.188e-14	7.863e-11	7.863e-11	2.776e-15
f_C	—	4.079e-12	4.053e-12	5.607e-14	3.088e-11	3.086e-11	8.898e-13
f_T	10^{-2}	2.270e-13	2.269e-13	9.717e-14	6.566e-14	6.584e-14	1.145e-13
f_T	10^{-4}	1.683e-07	1.476e-07	5.097e-14	5.176e-12	4.477e-12	1.033e-13
f_T	10^{-6}	5.348e-11	5.348e-11	1.048e-13	8.920e-06	9.010e-06	1.099e-13
f_L	10^{-2}	2.462e-09	2.460e-09	2.442e-15	1.415e-09	1.415e-09	3.331e-16
f_L	10^{-4}	3.437e-09	3.436e-09	1.332e-14	2.022e-09	2.022e-09	3.331e-16
f_L	10^{-6}	5.810e-09	5.808e-09	3.553e-15	4.774e-10	4.774e-10	4.441e-16
f_A	10^{-2}	2.031e-11	2.028e-11	1.157e-13	7.198e-12	7.203e-12	1.199e-14
f_A	10^{-4}	1.089e-06	1.091e-06	9.179e-14	1.344e-11	1.312e-11	1.573e-13
f_A	10^{-6}	1.235e-07	1.235e-07	4.963e-14	3.191e-10	3.033e-10	5.174e-14

Table 4 Experimental results for the interval $[-1, 1]$ and derivative order $m = 2$.

- the interpolation nodes of the rational approximant r , and
- the points $\pm 10^{-15}, \pm 10^{-14.9}, \pm 10^{-14.8}, \dots, \pm 10^{-3}$ away from each node (in an angular sense for the unit circle), inside the domain.

In our results, we report the maximum over T_f of three types of errors:

- The absolute error $|f^{(m)}(z) - r^{(m)}(z)|$ using our new algorithms, called *Formula* error in the tables;
- The same quantity computed using extended precision arithmetic (**Double64** from the `DoubleFloats.jl` package), called *Formula-EP* error; and
- The error in a discrete AAA or greedy TCF approximation to the exact $f^{(m)}$ evaluated at the test point set, called *Direct* error.

We expect to see a difference between *Formula* and *Formula-EP* errors only if the evaluation formula is numerically unstable. The purpose of reporting *Direct* errors is to estimate the best-case accuracy that can be expected from a rational approximant of the targeted derivative.

Tables 3 and 4 show results for the first and second derivatives on the interval $[-1, 1]$, while Tables 5 and 6 show results for the unit circle. In all cases, the *Formula* and *Formula-EP* errors are very close to one another, indicating that our derivative algorithms are stable for all the test cases considered. The *Direct* errors are often smaller than the formula errors, indicating that the accuracy of the derivative evaluation is limited by the conditioning of the problem, which typically worsens as singularities approach the domain of approximation. In particular, the test function f_L has derivatives that are a simple or double pole and thus have essentially no truncation error when approximated directly. But the derivative calculations from approximation of f_L itself involve the interaction of many poles that serve to approximate the branch cut of the logarithm.

Function		Barycentric			TCF		
Name	ϵ	Formula	Formula-EP	Direct	Formula	Formula-EP	Direct
f_E	—	3.049e-12	3.047e-12	8.019e-15	8.325e-13	8.323e-13	6.746e-14
f_C	—	4.375e-13	3.853e-13	1.746e-13	2.366e-12	2.348e-12	5.668e-13
f_M	—	3.939e-13	3.918e-13	2.004e-13	3.941e-13	3.876e-13	1.544e-14
f_L	10^{-2}	6.502e-12	6.508e-12	1.123e-15	6.558e-12	6.553e-12	4.336e-16
f_L	10^{-4}	2.337e-12	2.312e-12	5.804e-15	7.410e-12	6.796e-12	3.511e-16
f_L	10^{-6}	2.081e-09	8.495e-10	7.111e-14	7.090e-07	7.479e-07	2.776e-16
f_S	10^{-2}	9.811e-12	9.801e-12	1.441e-13	8.369e-12	8.386e-12	1.510e-13
f_S	10^{-4}	1.461e-10	1.456e-10	1.222e-12	2.542e-10	2.541e-10	9.580e-13
f_S	10^{-6}	6.364e-08	6.362e-08	1.016e-10	1.613e-09	1.568e-09	9.564e-11

Table 5 Experimental results for the unit circle and derivative order $m = 1$.

Function		Barycentric			TCF		
Name	ϵ	Formula	Formula-EP	Direct	Formula	Formula-EP	Direct
f_E	—	4.132e-11	4.131e-11	1.551e-14	1.217e-11	1.217e-11	2.210e-14
f_O	—	2.160e-12	2.038e-12	4.079e-13	1.147e-11	1.145e-11	2.179e-13
f_M	—	1.022e-12	1.021e-12	1.282e-13	1.330e-12	1.311e-12	5.964e-14
f_L	10^{-2}	7.357e-11	7.352e-11	6.206e-15	7.577e-11	7.577e-11	6.684e-16
f_L	10^{-4}	1.491e-10	1.488e-10	8.893e-16	1.030e-10	1.005e-10	6.474e-16
f_L	10^{-6}	9.220e-09	9.180e-09	5.445e-15	2.088e-08	1.170e-08	5.979e-16
f_S	10^{-2}	2.779e-10	2.781e-10	7.685e-14	1.803e-10	1.805e-10	1.169e-13
f_S	10^{-4}	5.647e-09	5.628e-09	3.568e-12	6.106e-09	6.107e-09	4.594e-12
f_S	10^{-6}	3.373e-08	3.359e-08	1.818e-10	3.877e-08	3.864e-08	4.326e-10

Table 6 Experimental results for the unit circle and derivative order $m = 2$.

5 Conclusions

We have demonstrated efficient, stable algorithms for evaluating the derivatives of rational functions in both barycentric and Thiele continued fraction representations. The proposed method for the barycentric representation is, to our knowledge, the first globally stable one. While we lack formal proofs of stability, numerical experiments on first and second derivatives confirm it for a variety of test functions and domains. We note that due to the conditioning of the problem, the accuracy obtainable for derivatives of rational approximations can be lower than for the approximations themselves, and for a direct rational approximation of the exact derivative function.

Accounting for the interpolation node nearest the evaluation point z via (13) seems to provide sufficient stability for evaluating the first two derivatives of a barycentric representation for all the experiments in section 4. In principle, though, z might be close to two or more nodes when the nodes are tightly clustered. If this proves to be a concern, one might need to resort to the much slower (8) for the first derivative and a triple sum for the second derivative, or find more sophisticated approximations, such as multipole expansions.

6 Data availability

No data were used in the research described in the article. Software implementing the algorithms described is available at <https://github.com/complexvariables/RationalFunctionApproximation.jl>.

References

[1] Nakatsukasa, Y., Sète, O., Trefethen, L.N.: The AAA algorithm for rational approximation. *SIAM Journal on Scientific Computing* **40**(3), 1494–1522 (2018) <https://doi.org/10.1137/16m1106122>

- [2] Nakatsukasa, Y., Trefethen, L.N.: Applications of AAA Rational Approximation. arXiv (2025). <https://doi.org/10.48550/arXiv.2510.16237>
- [3] Salazar Celis, O.: Numerical Continued Fraction Interpolation. Ukrainian Mathematical Journal **76**(4), 635–648 (2024) <https://doi.org/10.1007/s11253-024-02344-5>
- [4] Driscoll, T.A., Zhou, Y.: Greedy Thiele Continued-Fraction Approximation on Continuum Domains in the Complex Plane. arXiv (2025). <https://doi.org/10.48550/arXiv.2510.07295>
- [5] Schneider, C., Werner, W.: Some new aspects of rational interpolation. Mathematics of Computation **47**(175), 285–299 (1986) <https://doi.org/10.1090/S0025-5718-1986-0842136-8>
- [6] Jones, W.B., Thron, W.J.: Numerical stability in evaluating continued fractions. Mathematics of Computation **28**(127), 795–810 (1974) <https://doi.org/10.1090/S0025-5718-1974-0373265-5>
- [7] Higham, N.J.: Accuracy and Stability of Numerical Algorithms, 2nd edn. SIAM, Philadelphia, PA (2002)
- [8] Driscoll, T.A.: RationalFunctionApproximation.Jl: Rational Function Approximation in Julia. Zenodo (2023). <https://doi.org/10.5281/ZENODO.8355790>
- [9] Driscoll, T.A., Nakatsukasa, Y., Trefethen, L.N.: AAA Rational Approximation on a Continuum. SIAM Journal on Scientific Computing **46**(2), 929–952 (2024) <https://doi.org/10.1137/23M1570508>